

# Analysis of the Periodic Noise on In-Vehicle Broadband Power Line Channels

José Antonio Cortés, Miguel Cerdá, Luis Díez, Francisco Javier Cañete  
Departamento de Ingeniería de Comunicaciones  
E.T.S.I. de Telecomunicación (University of Málaga)  
Campus de Teatinos s/n, 29071 Málaga (Spain)

**Abstract**—Impulsive noise is probably the most harmful disturbance existing in the in-vehicle PLC scenario. Studies performed up to now have provided statistics of their pulse width, amplitude, bandwidth and interarrival time. However, they have disregarded the periodic behavior of most of them. In addition, their accuracy is strongly limited by the amplitude of the remaining noise terms. This paper presents a detailed analysis of the periodic noise terms (impulsive or not) that appear on in-vehicle power line channels in the band up to 25 MHz. The employed methodology detects and estimates their parameters even when their amplitude is much smaller than the one of the remaining noise components. This is carried out by exploring the harmonically related peaks that appear in the power spectral density when periodic noise terms are present.

**Index Terms**—Periodic impulsive noise, broadband, in-vehicle, power-line communications (PLC).

## I. INTRODUCTION

The number of electronic devices in vehicles has experienced an exponential growth in the last decades [1], [2]. Communication between the on-board electronic devices is currently accomplished by means of dedicated buses. The use of the power distribution lines inside vehicles also for communication purposes, the so-called power line communications (PLC), is a promising alternative that would reduce the vehicles price, due to the reduction in the wiring and its installation costs, and the fuel consumption and emissions, because of the reduction in the vehicles weight.

An adequate characterization of the existing noise in the in-vehicle power network is essential for the development of appropriate PLC systems. Most of the studies accomplished up to now have concentrated in the impulsive noise components, which are probably the most harmful ones for a communication system. Measurements have been accomplished by means of a digital oscilloscope (DSO). Different strategies are then applied to extract the impulsive components. In [3] impulses are detected by means of a peak detector. A more sensitive technique is proposed in [4]. It computes the cumulative variance of the noise sample amplitudes. This method is appropriate to detect impulses with amplitudes higher than tens of mV. However, since it operates in the time-domain, it may

have difficulties for detecting impulses with lower amplitudes than the existing narrowband interferences or background noise [5]. The periodical behavior of some impulses can be deduced from the statistics of the interarrival time. However, the method does not explicitly search for them.

A more complex impulse detection strategy based on the combination of hidden Markov models and maximum a posteriori, along with a frequency domain technique, is used in [6]. Unfortunately, provided results are limited to some examples. Interestingly, the authors report the presence of a particular impulsive noise term that they denote as “bursty waves”, and that in this paper are referred to as periodic waveforms.

This work presents an analysis of the periodic noise terms, i.e. periodic impulsive noise and periodic waveforms. It benefits from the resemblance between the in-vehicle PLC noise scenario and the indoor PLC one. The latter exhibits periodic impulsive noise terms with high repetition rates, the so-called periodic asynchronous impulsive noise, and low repetition rate terms, the so-called periodic synchronous impulsive noise. Algorithms for their respective analysis have been proposed in [7] and [8]. The one in [7] will be used in this work for the analysis of the periodic impulsive components that exhibit high repetition rates. However, the method proposed in [8] cannot be used to study the in-vehicle components with low repetition rates. The reason is that the repetition rate of the periodic synchronous noise is always a multiple of 50 Hz (in Europe), what simplifies the problem. Hence, a more elaborated method will be presented in this work.

The paper is organized as follows. The employed methodology is firstly described in section II. Representative examples of the waveforms and repetition rates, along with a summary of the main characteristics of the registered components, are provided in section III. Finally, conclusions are given in section IV.

## II. MEASUREMENT METHODOLOGY

The measurement setup consists of a computer with a 12-bit data acquisition board (DAB). It has a configurable dynamic range and an input impedance of 50  $\Omega$ . The DAB is plugged to the in-vehicle power network

through a coupling circuit that acts as a passband filter and as a balun that extracts differential mode signal [8]. The measured bandwidth extends up to 25 MHz. The captured data is real-time transferred to the computer, allowing recording lengths of 4.68 seconds.

This procedure has been employed to acquire 58 noise registers in the vehicles shown in Table I. At some measuring points only the feed wire is available (cars use to have earth return). In these cases, one of the coupling circuit terminals is connected to the nearest chassis point. Three different states have been considered: engine off (ignition switch off), engine off (ignition switch on) and engine idling. The number of active functions varies from one measurement to another: lighting system (driving, directional, brake and emergency lights), radio/CD, etc. Measurements have been accomplished at different points of the vehicle: lighter, rear light socket, fuse box and battery.

Table I  
DESCRIPTION OF VEHICLES

Vehicle	Model	Power (hp) / Displacement (cc)	Fuel	Year
1	Ford Mondeo	136 / 2000	Diesel	2004
2	Mazda MX5	110 / 1600	Petrol	2002
3	Fiat Punto	60 / 1200	Petrol	2002

#### A. Algorithm for extraction of periodic impulsive noise with high repetition rate

The key idea is to perform a high frequency resolution estimate of the power spectral density (PSD) of the noise register. Periodic noise terms will manifest in this estimate as harmonically related narrowband peaks. The time-domain waveform of the noise component can be extracted by means of a filter with multiple passbands, one for each narrowband peak [7]. A detailed description is given below.

The first step is to compute a high resolution spectral analysis based on periodogram averaging. The registered signal,  $x(n)$ , whose length is  $N_T$ , is divided into segments of length  $N_L$ ,

$$x_\ell(n) = x(n + \ell N_L), \quad (1)$$

with  $0 \leq n \leq N_L - 1$  and  $0 \leq \ell \leq L - 1$ , where  $L = \lfloor \frac{N_T}{N_L} \rfloor$ . The corresponding periodograms are then computed according to

$$P_\ell(k) = \frac{1}{UN_L} \left| \sum_{n=0}^{N_L-1} w(n)x_\ell(n)e^{-j\frac{2\pi}{N_L}kn} \right|^2, \quad (2)$$

where  $0 \leq k \leq N_L - 1$ ,  $w(n)$  is a Hanning window of  $N_L$  samples and  $U$  is the normalization factor that removes the estimation bias [9]. An estimate of the time and frequency sampled version of the noise

instantaneous PSD can then be obtained by performing an averaging of the periodograms in (2)

$$\hat{S}_N(k) = \hat{S}_N(f) \Big|_{f=\frac{k}{T_s N_L}} = \frac{1}{L} \sum_{\ell=0}^{L-1} P_\ell(k), \quad (3)$$

where  $T_s$  is the sampling period.

Now the spectral peaks observed in (3) are estimated by means of the method described in [7]. The result is a spectral mask,  $M^i(k)$ , whose value is 1 in the frequencies where spectral peaks due to the  $i$ th periodic component are present, and zero otherwise. The corresponding time-domain impulse waveform is then obtained as

$$p_\ell^i(n) = \text{IDFT} \{ M^i(k) \text{DFT} \{ x_\ell(n) \} \}, \quad (4)$$

where  $\text{DFT} \{ \cdot \}$  and  $\text{IDFT} \{ \cdot \}$  denote the  $N_L$ -point Discrete Fourier Transform and Inverse DFT, respectively. The presence of the impulses in the whole noise register can be corroborated by using the correlation.

The frequency resolution of the estimated PSD is determined by the value of  $N_L$ . Its selection results from the following trade-off. When it is high enough, periodic noise terms will manifest as harmonically related peaks. Otherwise they will be hidden by the background noise. However, if  $N_L$  is too high, the number of periodograms to be averaged may be too low and the variance of the estimated PSD increases. This variance may hide the presence of the spectral peaks caused by the periodic noise terms. In this work  $N_L = 10^5$ . This results in a frequency and time resolution of 2 kHz and 2 ms, respectively. Hence, terms with periods larger than 2 ms will be seen as aperiodic and should be extracted using the algorithm described in the next subsection.

#### B. Algorithm for extraction of periodic impulsive noise with low repetition rate

The employed technique has three phases. The first is aimed at determining the existence of low frequency components. To this end, the input signal is divided into a large number of segments of small duration and the periodogram of each segment is computed. Segments containing impulses whose period is larger than twice the segment duration will exhibit a much higher noise floor than the adjacent ones.

The second phase is aimed at computing the mask used to extract the pulse waveform detected in the previous phase. The high value of  $N_L$  that is required for this purpose prevent us from using the procedure described in the previous subsection. Hence, the process is performed in two steps. Firstly, a mask identifying all the periodic noise terms with high repetition rate and the narrowband interferences is computed using  $N_L = 10^5$ . Secondly, this mask is extrapolated to a value of  $N_L = 2 \cdot 10^6$ . The resulting mask

captures the spectral peaks due to the high repetition rate components and narrowband interferences, but it has no trace of the peaks due to components whose period is larger than  $10^5/2$  samples, i.e. repetition rates lower than 500 Hz. Therefore, the complementary mask extracts only these low repetition rate terms.

The third phase extracts the pulse waveform by using the mask as in (4). The detailed procedure is as follows.

- 1) *Compute the periodograms of  $x_\ell(n)$  using a high time resolution.* By fixing  $N_L = 10^4$  (0.2 ms), components with period higher than  $2 \times 0.2$  ms (repetition rate lower than 2.5 kHz) will cause a significant variation in the “noise floor” of successive periodograms,  $P_\ell(k)$ .
- 2) *Reduce the variance of the periodograms.* The variance of the periodograms,  $P_\ell(k)$ , is high because no averaging has been accomplished. To reduce it, a median filtering is applied in the variable  $k$ . A sliding window with 100 samples ( $2 \mu\text{s}$ ) is employed for this purpose. The output of this step is  $\overline{P}_\ell(k)$ .
- 3) *Identify the spectral bands where  $\overline{P}_\ell(k)$  exhibits significant level differences when moving along the variable  $\ell$ .* Segments with higher values of  $\overline{P}_\ell(k)$  than the adjacent ones in some bands contain either aperiodic impulses or impulses from a low frequency component.
- 4) *Obtain a high frequency resolution estimate of the noise PSD and calculate the mask,  $M(k)$ , that identifies all the significant peaks in it.* A high frequency resolution estimation,  $\widehat{S}_N(k)$ , is obtained using expressions (1), (2) and (3) with  $N_L = 10^5$ . The mask,  $M(k)$ , is then obtained only for the frequency bands identified in step 3).
- 5) *Extrapolate  $M(k)$  to obtain a new mask,  $\widehat{M}(k)$ , with higher frequency resolution.* The increased frequency resolution is obtained by fixing  $N_L = 2 \cdot 10^6$ , and the new mask holds  $\widehat{M}(k \frac{2 \cdot 10^6}{10^5}) = M(k)$ .
- 6) *Obtain the pulse waveform.* This is accomplished by applying the complementary mask of  $\widehat{M}(k)$  to segments of length  $N_L = 2 \cdot 10^6$ ,

$$p_\ell(n) = \text{IDFT} \left\{ \left( 1 - \widehat{M}(k) \right) \text{DFT} \{ x_\ell(n) \} \right\}. \quad (5)$$

$p_\ell(n)$  contains the pulse waveforms of all the impulsive noise terms with low repetition rate that are present in each segment.

### III. MEASUREMENTS RESULTS

The proposed method is able to extract impulsive components that can be detected neither by a classical method based on a peak detector nor by the method proposed in [4]. This can be observed in Fig. 1 (a) and (b). The former depicts the time-domain plot of a 50  $\mu\text{s}$  segment of a noise register acquired in car 1. Two impulses are clearly visible, one around 5  $\mu\text{s}$

and another around 39  $\mu\text{s}$ . Fig. 1 (b) depicts the 64.82 kHz periodic impulsive noise component retrieved with the algorithm presented in section II-A. It is worth noting that each period (15.427  $\mu\text{s}$ ) is composed of two slightly different impulses with approximate lengths of 1.1 and 1.5  $\mu\text{s}$ , respectively. The cumulative variance proposed in [4] has been depicted for reference. To ease the comparison, a vertical offset and scaling has been applied to it. As seen, most of the impulses of the component are not visible in Fig. 1 (a) because they are masked by the narrowband interferences and the background noise. Similarly, many of these impulses do not cause an important change in the cumulative variance, e.g. the one around 2, 30 and 40  $\mu\text{s}$ .

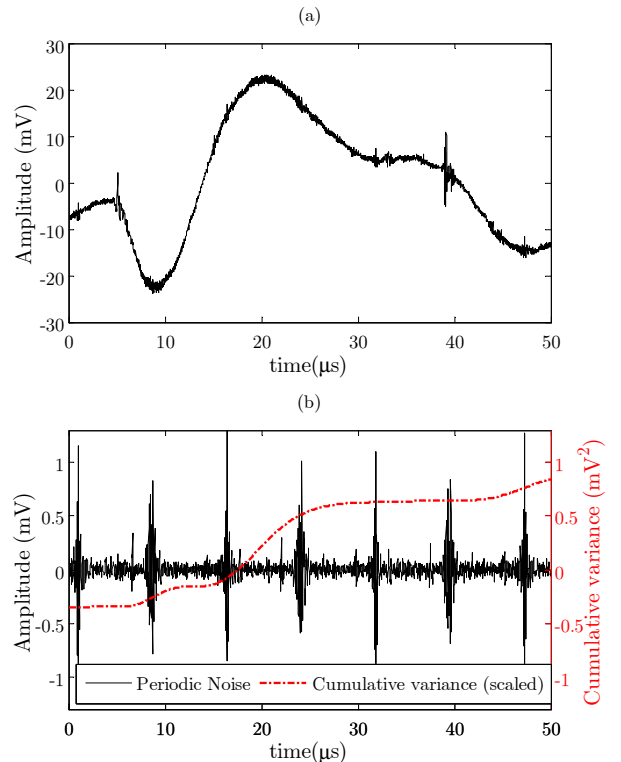


Figure 1. (a) Time-domain plot of a noise register segment; (b) Periodic noise component retrieved with the algorithm proposed in section II-A and cumulative variance (scaled).

It is worth noting that, despite the low amplitude of the periodic component in Fig. 1 (b), it can be very harmful for a communication system. Since their power is concentrated at certain frequencies, its PSD is many dB above the background noise level. This is illustrated in Fig. 2 (a) and (b), where the estimated PSD of the noise register is shown.

The proposed method is able to extract periodic impulsive noise components with overlapped bands and with very similar repetition rates. As an example Fig. 3 (a) shows a detail of the estimated PSD of a noise register captured in car 2. Fig. 3 (b) and (c) depict approximately one period of the waveforms

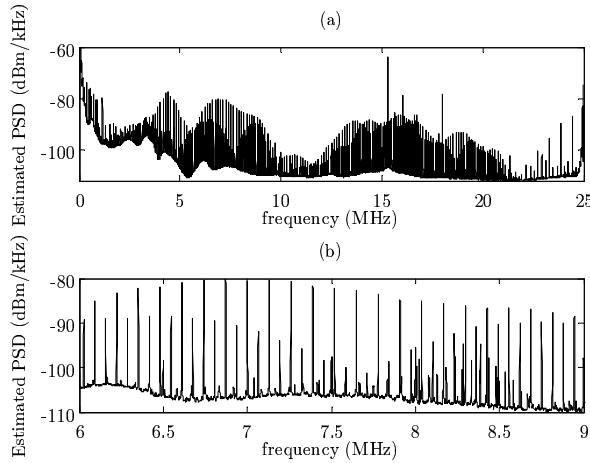


Figure 2. (a) Estimated PSD of the overall noise register partially shown in Fig. 1 (a); (b) Detail of the estimated PSD in (a).

corresponding to the pairs of spectral peaks shown in Fig. 3 (a). In both cases, each period is composed of two clearly different impulses. The repetition rates are 64.4175 kHz for the ones in Fig. 3 (b) and 64.4405 kHz for the ones in Fig. 3 (c). The difference between these repetition rates is only 23 Hz, which seems to be contradictory with the 2 kHz frequency resolution used to estimate the PSD. However, the spectral peaks shown in Fig. 3 (a) have harmonic indexes around 250 ( $16.15 \text{ MHz}/64.4175 \text{ kHz}=250.7083$ ). Hence, the frequency difference between the 250-th harmonics of the two impulsive components is 5.75 kHz, which is well beyond the frequency resolution.

#### A. High repetition rate impulsive noise

A common periodic noise component with a repetition rate of approximately 64.75 kHz (with variations of up to hundreds of Hz between cars) has been found in the noise registers captured in the three cars in all the engine states. It occupies almost the whole band and is usually the one with the largest level above the background noise. Pulses amplitude in car 2 are generally ten times larger than in the others. Fig. 3 (b) and (c) show an example of pulses waveform from this car.

Fig. 4 (a) depicts the pulse waveform of a periodic component with a repetition rate of 83.33 kHz, and Fig. 4 (b) plots the pulse waveform of a periodic component with a repetition rate of 129.52 kHz, which is the highest one found in the measurements. Fig. 4 (c) depicts the normalized Energy Spectral Density (ESD) of the pulses, defined as

$$ESD(f) = 20 \log_{10} \left( \frac{|P(f)|}{\max\{|P(f)|\}} \right) \quad (\text{dB}), \quad (6)$$

where  $P(f)$  is the Fourier transform of the pulse waveform,  $p(t)$ , in volts. As seen, impulses in Fig. 4

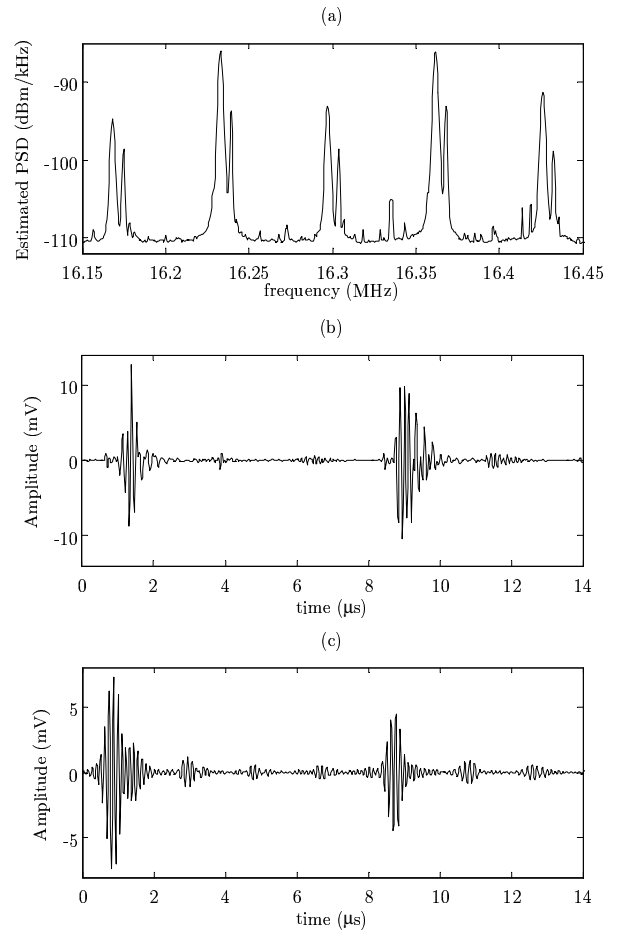


Figure 3. (a) Detail of the estimated PSD of a noise register; (b) Periodic noise term with frequency 64.417 kHz; (c) Periodic noise term with frequency 64.440 kHz.

(a) have significant ESD levels in a continuous band, whereas the ESD of the impulse in Fig. 4 (b) occupies a narrower band but split in two parts.

Table II summarizes the characteristics of the high repetition rate terms found in the three cars. The number of periodic terms with high repetition rates varies from one (engine off) up to 5 (surprisingly not with engine idling, but with engine off and ignition switch on). As seen, the repetition rates are in the order of the symbol periods used by current commercial broadband PLC systems employed in the indoor scenario (e.g., the symbol rate of the HomePlug AV is approximately 24.4 kHz). They may be caused by the CAN bus signals, whose bit rates may range from approximately 115 kbit/s up to 1 Mbit/s, or by the LIN bus, whose bit rate is 19.2 kbit/s. However, since in a first instance in-vehicle PLC are proposed as a redundant path for these conventional communication networks, coexistence between them will be required.

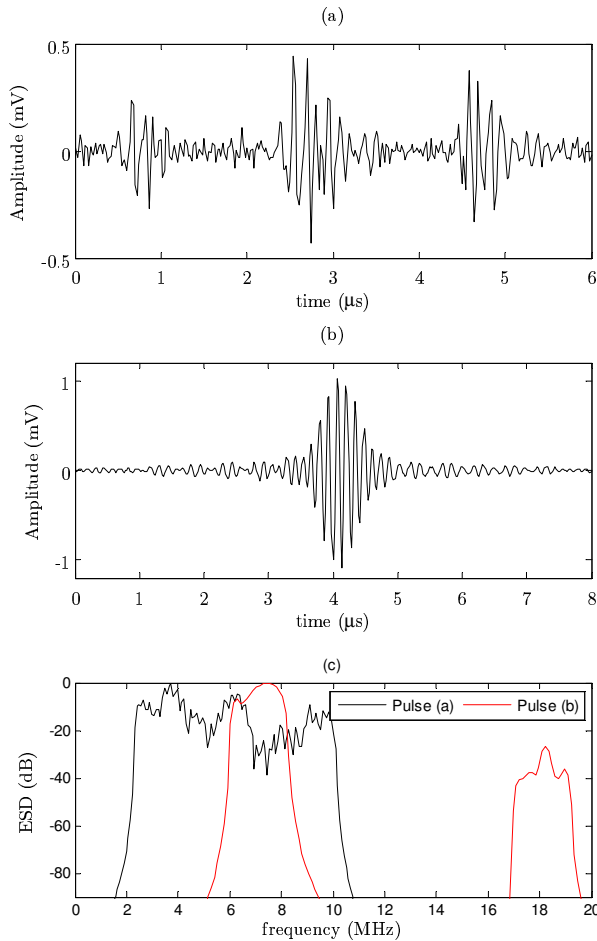


Figure 4. (a) Periodic noise component with a repetition rate of 83.33 kHz; (b) Periodic noise component with a repetition rate of 129.52 kHz; (c) ESD of the pulses in (a) and (b).

Table II  
CHARACTERISTICS OF PERIODIC IMPULSIVE NOISE WITH HIGH REPETITION RATES

Parameter	Value
Number of components	from one up to five, depending on the activated functions
Approximate duration	typically less than 2 μs, occasionally up to 4 μs
Amplitude	typically less than 2 mV, occasionally up to 20 mV
Repetition rates	15.68 kHz, 42.72 kHz, 63.93 kHz, 64.75 kHz, 83.33 kHz, 124.21 kHz, 128.8 kHz, 129.52 kHz
Central frequency	from 11 MHz up to 19 MHz
Bandwidth	from 1 MHz up to 22 MHz

### B. Low repetition rate impulsive noise

A periodic impulsive noise component with a repetition rate of 60 Hz has been found in the three cars in some of the considered working conditions and in most of the measurement points. Their amplitude and pulse

waveform depends on the car and on the measurement point. As an example, Fig. 5 (a) depicts the pulse waveform obtained in car 2. Fig. 5 (b) shows the pulse waveform of the periodic component with the lowest repetition rate that we have found, 26 Hz. Fig. 5 (c) plots the pulse waveform of a periodic term with a repetition rate of 3.51 kHz.

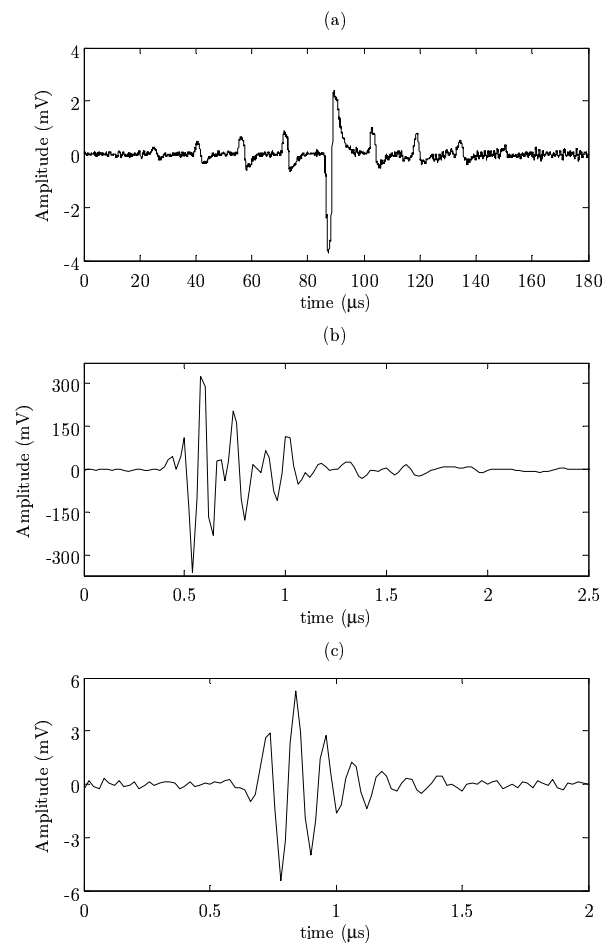


Figure 5. Periodic noise component with a repetition rate of: (a) 60 Hz; (b) 26 Hz and (c) 3.51 kHz.

Table III summarizes the characteristics of the components retrieved from the three cars. It is interesting to highlight the wide range of repetition rates. Most of them are quite low but, despite this fact, the occupied bandwidth may be located in a frequency band has high as 19.5 MHz.

### C. Periodic waveforms

Periodic components that do not have an impulsive nature have been also found in the measurements. They take the form of periodic signals with frequencies ranging from tens of kHz up to a few hundreds of kHz. They have a low-pass spectra that is usually located below 4 MHz. Their difference with the periodic im-

Table III  
CHARACTERISTICS OF PERIODIC IMPULSIVE NOISE WITH LOW REPETITION RATES

Parameter	Value
Number of components	from one up to four, depending on the activated functions
Approximate duration	typically less than 4 $\mu$ s, occasionally up to 240 $\mu$ s
Amplitude	typically less than 6 mV, occasionally up to 500 mV
Repetition rates	26 Hz, 44.6 Hz, 50 Hz, 60 Hz, 79.5 Hz, 100 Hz, 146 Hz, 172.1 Hz, 250.12 Hz, 400 Hz, 1.05 kHz, 3.5 kHz, 3.86 kHz
Central frequency	from 250 kHz up to 19.5 MHz
Bandwidth	from 500 kHz up to 12 MHz

pulsive noise terms is that the “pulse” duration equals the interarrival time.

As an example, Fig. 6 depicts a 77.5 kHz periodic waveform that has been found in car 1 in three measurement points and with different engine states. These waveforms may be the result of filtering the waveform generated by an onboard electronic device with the different channel responses existing from this device to the measurement points. It should be mentioned that the low order harmonics may have been affected by the high-pass effect of the coupling circuit, whose cut-off frequency is below 500 kHz.

#### IV. CONCLUSION

This paper has presented a detailed analysis of the periodic noise on in-vehicle power lines in the frequency band up to 25 MHz. The employed methodology exploits the harmonically related peaks that appear in the estimated PSD when periodic noise components are present. It allows retrieving the pulse waveform and the repetition rate, even when its amplitude is much smaller than the one of the remaining noise terms.

Representative pulse waveforms, along with a summary of their main characteristics, have been given. It has been found that the number of periodic components varies from one or two (when the engine is off) up to 7. Two of them have been found in all the vehicles.

#### ACKNOWLEDGMENT

This work has been partially supported by the Junta de Andalucía under Project TIC-03007.

#### REFERENCES

- [1] G. Leen and D. Hefferman, “Expanding automotive electronic systems,” *IEEE Computer*, vol. 35, no. 1, pp. 88–93, 2002.
- [2] A. J. Van Rensburg and H. C. Ferreira, “Automotive power-line communications: Favourable topology for future automotive electronic trends,” in *Proceedings of the International Symposium on Power Line Communications and its Applications (ISPLC)*, 2003, pp. 103–108.
- [3] W. Gouret, F. Nouvel, and G. El-Zein, “Powerline communication on automotive network,” in *Proceedings of the IEEE Vehicular Technology Conference (VTC)*, 2007, p. 25452549.

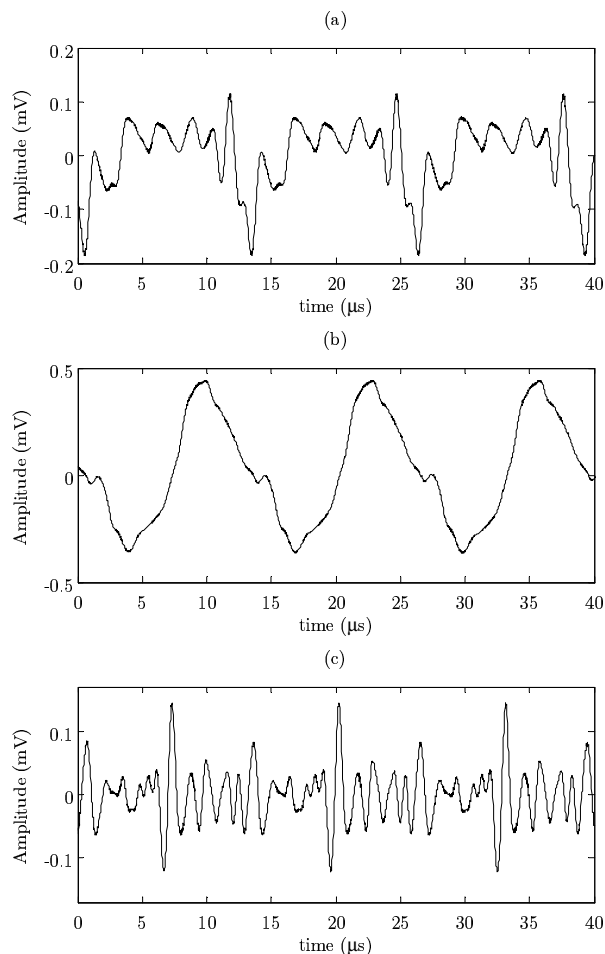


Figure 6. Periodic waveform with frequency 77.4 kHz registered in the same car in three different points and conditions: (a) rear brake light socket (engine idling); (b) fuse 1 in fuse box (engine idling); (c) fuse 2 in fuse box (engine off-ignition switching on).

- [4] V. Degardin, P. Lienard, M. Degauque, E. Simon, and P. Laly, “Impulsive noise characterization of in-vehicle power line,” *IEEE Transactions on Electromagnetic Compatibility*, vol. 50, no. 4, pp. 861–868, 2008.
- [5] F. Rouissi, V. Dégardin, M. Liénard, and P. Degauque, “Low amplitude impulsive noise in vehicular power line network,” in *Proceedings of the International Conference on Intelligent Transport Systems Telecommunications (ITST)*, 2009, pp. 538–542.
- [6] Y. Yabuuchi, D. Umehara, M. Morikura, T. Hisada, S. Ishiko, and S. Horiata, “Measurement and analysis of impulsive noise on in-vehicle power lines,” in *Proceedings of the IEEE International Symposium on Power Line Communications and Its Applications (ISPLC)*, 2010, pp. 325–330.
- [7] J. A. Cortés, L. Díez, F. J. Cañete, and J. López, “Analysis of the periodic impulsive noise asynchronous with the mains in indoor PLC channels,” in *Proceedings of the IEEE International Symposium on Power Line Communications and its Applications (ISPLC)*, March-April 2009, pp. 26–30.
- [8] J. A. Cortés, L. Díez, F. J. Cañete, and J. J. Sánchez-Martínez, “Analysis of the indoor broadband power-line noise scenario,” *IEEE Transactions on Electromagnetic Compatibility*, vol. 52, no. 4, pp. 849–858, Nov. 2010.
- [9] A. Oppenheim, R. Schaffer, and J. Buck, *Discrete-time Signal Processing*. Prentice Hall, 1999.